Copyright © 2016 by Academic Publishing House *Researcher*

Published in the Russian Federation
Nanotechnology Research and Practice
Has been issued since 2014.
ISSN: 2312-7856
E-ISSN: 2413-7227
Vol. 11, Is. 3, pp. 98-105, 2016

DOI: 10.13187/nrp.2016.11.98
www.ejournal13.com

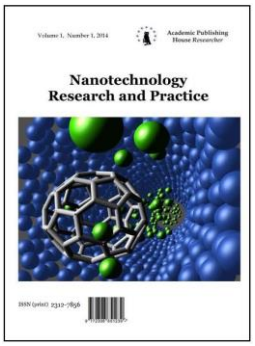

Articles and statements

UDC 620.3

Synthesis, Characterization of Nano Tin Oxide via Co-precipitation Method

K. Sujatha [a], T. Seethalakshmi [b], O.L. Shanmugasundaram [c]

[a] Department of Physics, Vellalar College for Women, Erode, Tamilnadu, India
PhD (Physics), Assistant Professor
E-mail: drsujiols@gmail.com
[b] Department of Physics, Karur Government College, Karur, Tamilnadu, India
Dr. (Physics), Associate Professor
E-mail: seethabala@gmail.com
[c] Department of Textile Technology, K.S. Rangasamy College of Technology, Tamilnadu, India
Dr. (Textile technology), Professor
E-mail: mailols@yahoo.com

Abstract

Pure SnO_2 nano powders were synthesized by co-precipitation method. The structure, surface, optical, and functional groups were analyzed by X-ray diffraction, FESEM, UV-Vis spectroscopy, FTIR and fluorescence spectra, respectively. The results were compared with pure tin oxide nanoparticle. X-ray analysis shows that the obtained power has tetragonal rutile structure with average crystallite size of 34 nm. Band gap is observed from UV-Vis spectroscopy. Fluorescence spectrum of pure sample detected a strong emission peaks at 634nm due to surface defect and oxygen vacancies in SnO2 nanoparticles.

Keywords: $SnCl_4$, nanopowder, co-precipitation method, FESEM, UV, XRD, SEM.

1. Introduction

Cassiterite structure Tin oxide (SnO_2) is a wide band gap (3.6-3.8 eV) [1-3] n type semiconductor. It has been most widely used semiconductor oxides because of its chemical and mechanical stabilities. Tin dioxide (SnO_2) is widely used in many applications such as catalysts agent [4, 5], hazardous gas sensors [6, 7], heat reflecting mirrors [8, 9], varistors [10, 11], transparent conducting electrodes for solar cells [12, 13], and optoelectronic devices [14].

Sensors consist of fine particles of metal oxides which exhibit high sensitivity. The factors affecting the sensitivity of the sensor is the crystallite size of the sensing materials. In order to achieve high sensitivities [5] semiconductor based sensors have fine crystallites. For the synthesis of SnO_2 nanostructures, many processes have been developed, e.g., spray pyrolysis, hydrothermal methods, chemical vapor deposition, thermal evaporation of oxide powders and sol–gel method [15-20].

In the present work, SnO_2 nanoparticles were synthesised by Co-precipitation method. The objective of this work is to determine the influences of the structure, optical and surface morphology of prepared SnO_2 nano powder. The crystalline structure of pure SnO_2 nano powder was characterized by X-ray powder diffraction (XRD). The surface morphology of the samples was recorded using FESEM, optical characteristics were verified by UV-Vis measurement and functional group was analyzed by FTIR spectrometer.

2. Discussion

Experimental Procedure

For the preparation of nano structured SnO_2 powder, 4 g tin (II) tetrachloride was dissolved in 200ml distilled water under vigorous stirring for 20 minutes. Aqueous ammonia was added drop wise to the resulting solution in order to modulate the pH at 12. The solution was then left for constant stirring for about 30 minutes. The solution was then left for constant stirring for about 30 minutes. The precipitate was collected and washed with de-ionized water. After drying at 100°C in oven for 24 hours, the SnO_2 nano particles was obtained and it was annealed at 500°C in furnace for 2 hours.

The samples were characterized by XRD, Scanning Electron Microscopy, Fourier transform Infra-red spectroscopy (FTIR), particle size analyser and fluorescence spectra.

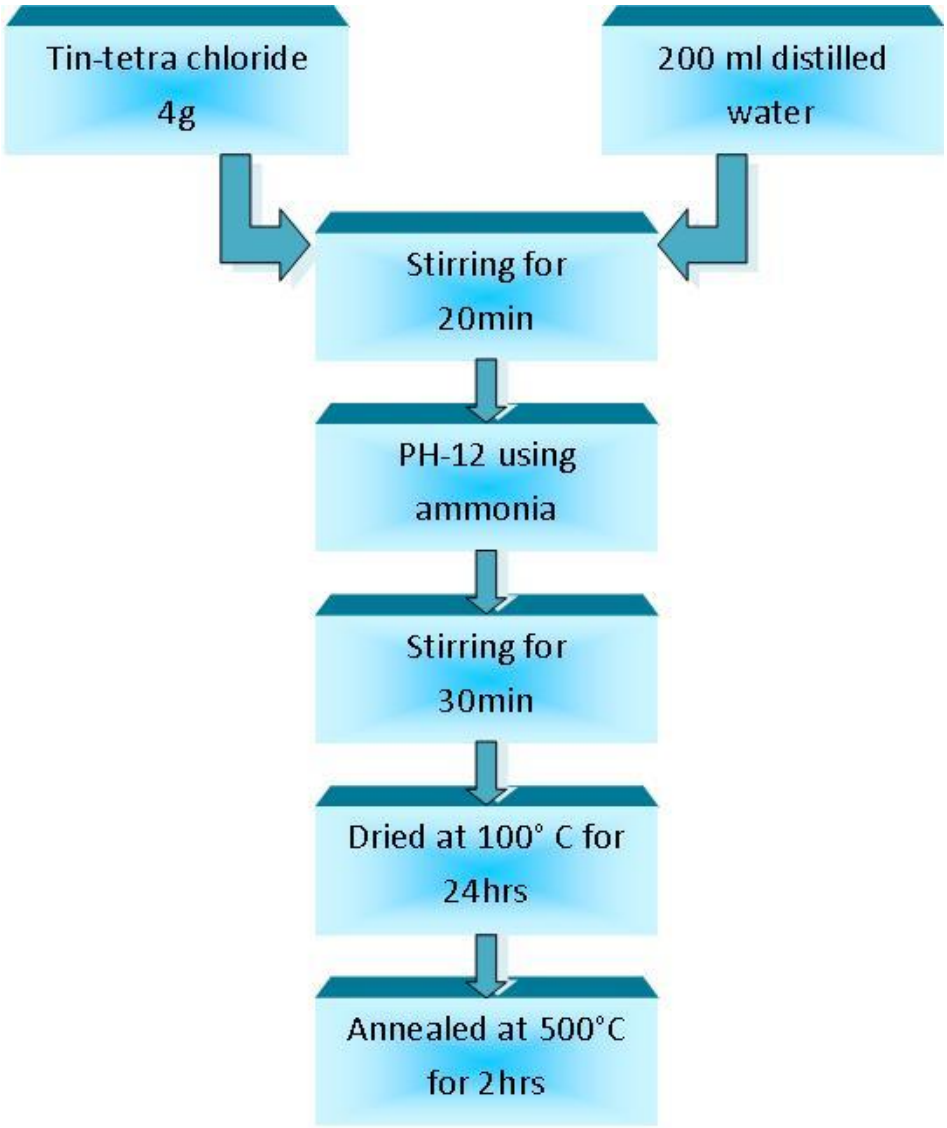

Fig. 1. Diagram of Preparation method of nano SnO_2

Characterization and Discussion of Results

1. X ray diffraction (XRD)

Using X-ray diffraction, Phase analysis was studied. The average crystallite sizes of the nano particles were calculated based on Scherer's equation [21, 22].

$$D = \frac{K\lambda}{\beta \cos\theta} \quad (1)$$

Where, D is the mean crystallite size, K is the shape factor taken as 0.89, λ is the wavelength of the incident beam, β is the full width at half maximum and θ is the Bragg angle.

$$2d_{hkl} \sin(\theta) = m\lambda \quad (2)$$

Where d is the spacing between the planes in the atomic lattice. h, k, and l are all integers, (hkl) is the lattice plane index, a and c are lattice constants, d_{hkl} is the distance between two consecutive planes (m=1) with plane index (hkl). The lattice parameter a and c of the SnO2 nano particle and volume of the tetragonal structure SnO2 were calculated using the standard equation [4].

$$\frac{1}{d^2} = \frac{h^2 + k^2}{a^2} + \frac{l^2}{c^2} \quad (3)$$

The obtained rutile structure was compared with JCPDS data (Card No. 41-1445). The pure SnO_2 sample shows 3 major peaks appear at 26.5836°, 33.8611° and 51.7775°, respectively.

All the observed peaks in the XRD pattern gives peak position, Miller indices, interplanar distances (observed and standard) their deviation and the microstrain of the particles.

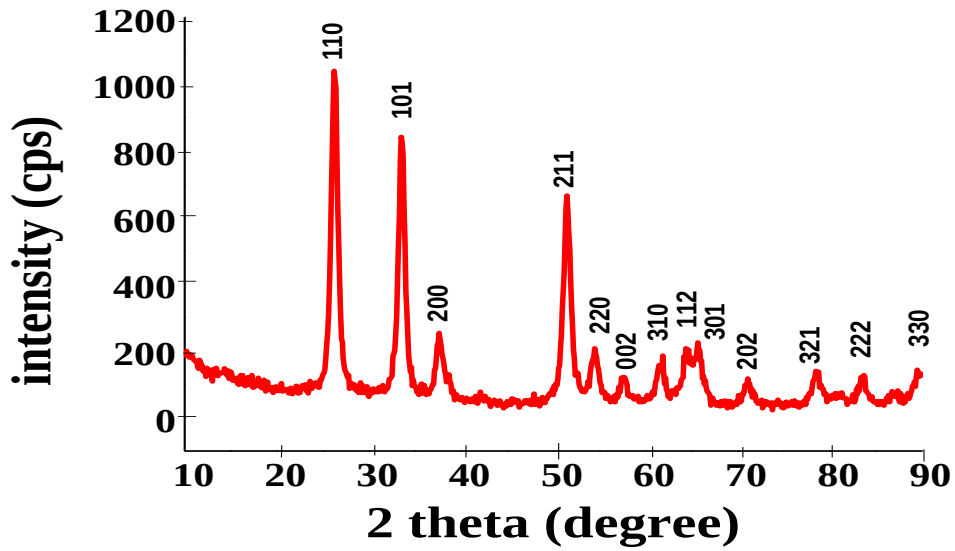

Fig. 2. XRD pattern of Pure SnO_2 powder

Table 1. Interplanar d_{hkl} spacings and microstrain in the SnO_2 nanopowder

2Theta	(hkl)	Interplanar distance (dhkl) (Å)		Deviation in dhkl = d_o-d_s (Å)	MicroStrain ε =Δd_{hkl} /d_s
		Obs (d_o)	Std (d_s)		
26.2291	110	3.39491	3.3370	0.05791	0.01735
33.5268	101	2.67076	2.6427	0.02806	0.01061
37.6366	200	2.38802	2.3690	0.01902	0.00802
51.4779	211	1.77377	1.7641	0.00967	0.00548

54.4341	220	1.68422	1.6750	0.00922	0.00550
57.5619	002	1.59992	1.5934	0.00652	0.00409
61.6104	310	1.50414	1.4984	0.00574	0.00383
64.4000	112	1.44555	1.4392	0.00635	0.00441
65.6000	301	1.42198	1.4155	0.00648	0.00457
71.0316	202	1.32598	1.3220	0.00398	0.003010
71.7000	320	1.31526	1.3141	0.00116	0.00882
78.5250	321	1.21715	1.2147	0.00245	0.00201
83.4403	222	1.15749	1.1544	0.00309	0.0026

Table 2. Unit Cell Parameters of the as-synthesized SnO_2 powder

Unit Cell Parameters	Calculated (110)Peak Crystal size(D)(nm)	JCPDS [41-1445]	Cell Refinement
Lattice constant a (Å) = b(Å)	a =4.7422A^0	a =4.7382A^0	4.7409504
c = (Å)	c= 3.1908 A^0	c = 3.1871 A^0	3.1885963
Axial Ratio a/c	1.4862	1.4866	1.48684560
Axial Ratio c/a	0.6728	0.6726	0.6725647
Volume $V=a^2c$	71.756	71.55	71.66884

By accurately measuring the d-values of (110) and (101) peaks, obtained values are tabulated as in Table 2. These values are again verified by use of the cell refinement software for the same tetragonal structure by considering all the indexed peaks.

Obtained values a = 4.7422Å and C = 3.1908 Å are matched with the standard JCPDS [41-1445]values. Similarly, refined cell constant exactly matches with the standard value and is in agreement with the reported values. The unit cell volume of the Tetrogonal system is,

$$V= a^2c \quad (4)$$

The calculated and refined values of unit cell volume of the crystal system, shown in Table 3 also matches well with the standard values.

Table 3. Crystallite and particle size of nanocrystalline SnO_2 powders

Sample	$D = \frac{K\lambda}{\beta\cos\theta}$ (nm)	a (Å)	c (Å)	S =6/ρD (m2/g)
SnO2	34.8420	a =4.7422A^0	c= 3.1908 A^0	6.994

2. Fourier Transform Infrared (FTIR) spectroscopy

Functional groups were investigated using spectrometer [23] in the range from 4500–400cm^{-1} at the resolution of 3cm^{-1}. Spectra were measured in the transmission mode.

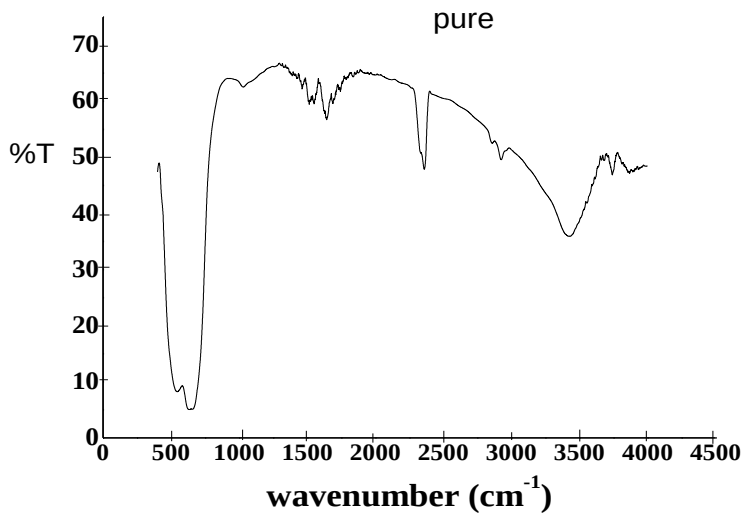

Fig. 3. FTIR spectra of Pure SnO_2 nanoparticles

The spectrum of tin oxide exhibited the main characteristic peak at 1743.66, 1551.26, 633.62 and 542.46cm$^{-1.}$ The strong broad peak centered at 633.62 cm^{-1} corresponds to Sn-O-Sn stretching vibration. The peak around 1400 cm^{-1} was assigned to NH stretching vibration from decomposition of NH_3. The bands at around 600 and 550 cm^{-1} were attributed to Sn-O stretching modes of Sn-O-Sn and Sn-OH respectively. The peaks in the FTIR spectrum at about 3300-3400 and 1645-1620 were due to stretching vibrations of water molecules absorbed at the surface of the tin oxide.

3. Scanning Electron Microscope (SEM)

The SEM micrographs (Fig. 4), the nanopowders are in mostly spherical in shape and agglomerate crystal size of 0 .2 μm. Agglomeration is due to strong hydrogen bonding in the network. In Fig. 4(a), the synthesized sample consists of fine tiny nanoparticles and the surface of the nanoparticle is approximately homogeneous with some agglomerates.

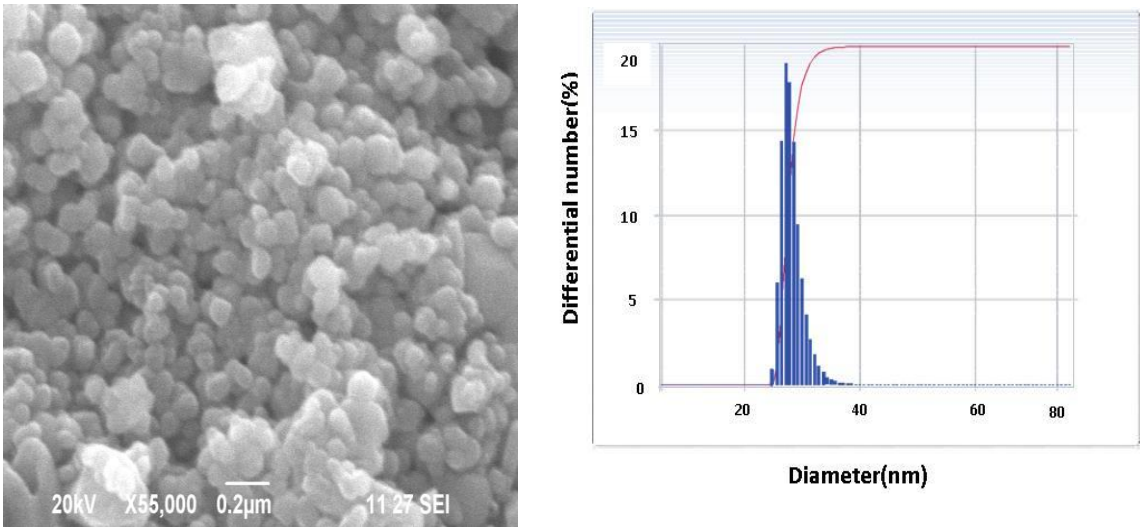

Fig. 4. (a) SEM (b) Particle size analyser of SnO_2 powder

The average particle size is determined from SJC Size Method, is about 27 nm, as shown in Fig. 4(b). The results are obtained from the SJC Size Method of the SnO2 nanoparticles show that the histogram of the percentage of SnO2 as a function of the grain size as in the Fig. 4.

4. UV/Vis/NIR absorption spectra

UV/Vis/NIR absorption spectra of samples were recorded at room temperature with a wave length range from 200 to 1200 nm. Fig.5 shows the optical absorption spectra of the pure SnO_2 nanoparticles.

The UV–vis absorption spectra of SnO_2 nanoparticles were analyzed and the result was displayed in figure 5. The absorption bands exhibited in the ultraviolet wavelength region which is near the visible-light range.

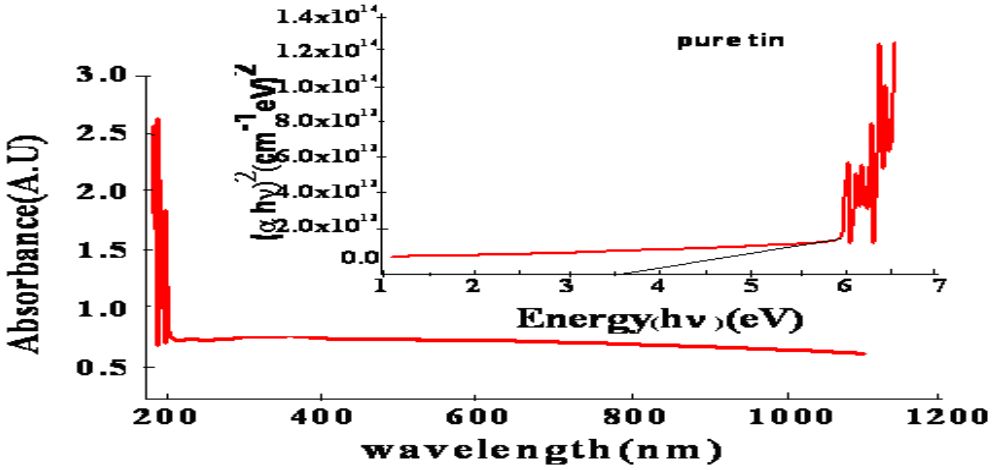

Fig. 5. UV/Vis/NIR absorption spectra with pure SnO_2 nanoparticles and $(\alpha h\nu)^2$ versus hν plot (inset)

Using Tauc Plot, the band gap was found to 3.5 eV by linear fitting, the absorption band edge in the plot of $(\alpha h\nu)^2$ versus hν plot. The resultant value of E_g shows a good agreement with the values published by other workers [24, 25].

5. Transmittance spectra

UV/Vis/NIR transmittance spectra of samples were recorded at room temperature with a wave length range from 190 to 1000 nm. Cut off wavelength of SnO_2 nanoparticle is 200 nm which is observed from transmittance spectrum.

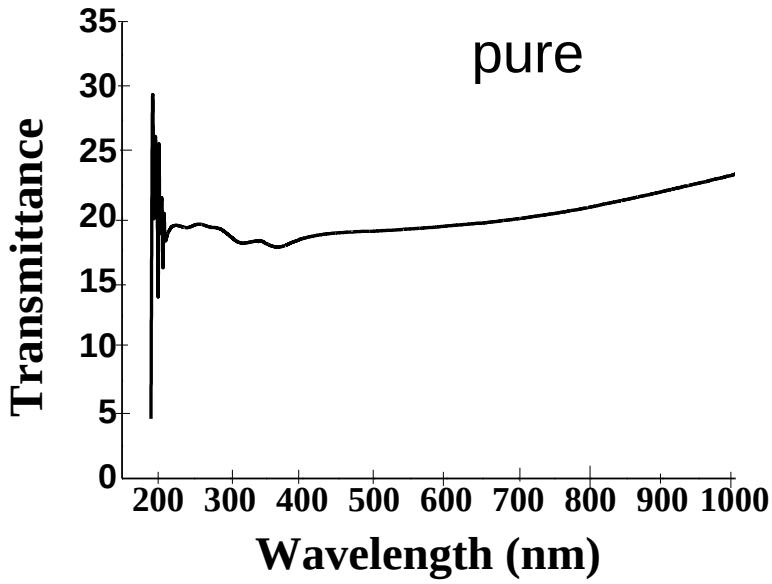

Fig. 6. UV/Vis/NIR Transmittance spectra with pure SnO_2 nanoparticles

6. Fluorescence spectrum

Fluorescence spectrum was measured with excitation wavelength of 300 nm. Fig. 7 shows spectrum of pure sample detected a strong emission peak at 634 nm due to the surface defect and oxygen vacancies in SnO_2 nanoparticles.

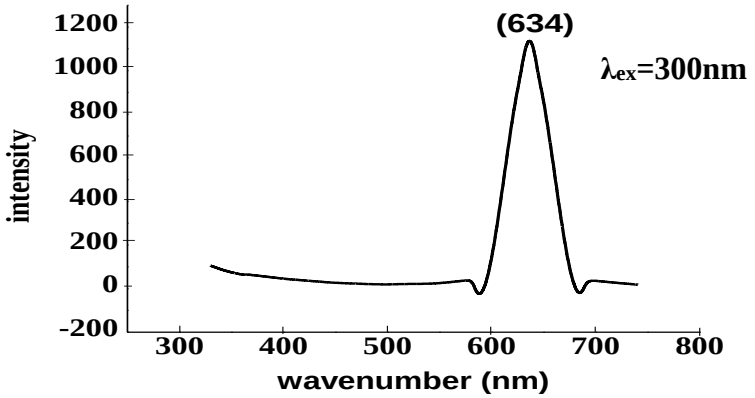

Fig. 7. Fluorescence Spectra of Pure SnO_2 Nanoparticles

The intensity of emission peak may vary based on sample's particle size.

3. Conclusion

In summary, pure SnO_2 nanopowders with tetragonal phase were synthesized by co-precipitation method. The XRD patterns exhibited the rutile type tetragonal structure of pure samples and no impurity phase was observed in XRD. The crystallite size of pure tin oxide was 34 nm. Surface morphology of nano particles showed fine tiny nanoparticles with certain agglomeration. The optical properties were studied using UV-Vis spectroscopy which suggested the band gap is found to be 3.5 eV. The Fluorescence spectrum study exhibit an emission centre at 634nm pointed a red light emission.

References

1. E. Ganesh Patil, D.D. Kajale, D.N. Chavan, N.K. Pawar, P.T. Ahire, S D Shinde, V.B. Gaikwad, G.H. Jain. Synthesis, characterization and gas sensing performance of sno2 thin films prepared by spray pyrolysis. Bull. Mater. Sci., Vol. 34, No. 1, pp. 1–9. February 2011.

2. L.C. Nehru, V. Swaminathan, C. Sanjeeviraja. Photoluminescence Studies on Nanocrystalline Tin Oxide Powder for Optoelectronic Devices. American Journal of Materials Science, Vol.2, No.2, pp. 6-10, 2012.

3. S. Gnanam, v. Rajendran. Luminescence properties of eg-assisted sno2 nanoparticles by sol-gel process", Digest Journal of Nanomaterials and Biostructures, Vol. 5, No 3, pp.699-704, July-September 2010.

4. L. Chou, Y. Cai, B. Zhang, J. Niu, S. Ji, S. Li. Influence of SnO2-doped W-Mn/SiO2 for oxidative conversion of methane to high hydrocarbons at elevated pressure. Appl. Catal. A: Gen. 238.pp185-191 (2003).

5. P.T. Wierzchowski, L.W. Zatorski. Kinetics of catalytic oxidation of carbon monoxide and methane combustion over alumina supported Ga2O3, SnO2 or V2O5. Appl. Catal. B: Environ. 1352, pp. 1-8 (2003).

6. A.J. Moulson, J.M. Herbert. Electroceramics – Materials, Properties, Applications, (Chapman & Hall, London, 1990).

7. Y. Shimizu, M. Egashira. Basic Aspects and Challenges of Semiconductor Gas Sensors MRS Bull. 24,14-24 (1999) 18.

8. M. Kojima, F. Takahashi, K. Kinoshita, T. Nishibe, Ichidate. Transparent furnace made of heat mirror. Thin Solid Films 392, pp. 349-354 (2001).

9. C.M. Lampert. Heat mirror coatings for energy conserving windows. Solar Energy. Materials. Vol 6 (1981), Is. 1.

10. J.F. Wang, Y.J. Wang, W.B. Su, H.C. Chen, W.X. Wang. Novel (Zn, Nb) – doped SnO2 varistors. Mater. Sci. Eng. B 96, pp. 8-13 (2002).

11. M.R.C. Santos, P.R. Bueno, E. Longo, J.A. Varela. Effect of oxidizing and reducing atmospheres on the electrical properties of dense SnO_2-based varistors. Eur. Ceram. Soc. Vol 21(2001) 161-167, Is. 2.

12. T.E. Moustafid, H. Cachet, B. Tribollet, D. Festy. Modified transparent SnO2 electrodes as efficient and stable cathodes for oxygen reduction. Electrochimica Acta, 47(8), pp. 1209–1215.

13. M. Okuya, S. Kaneko, K. Hiroshima, I. Yaggi, K. Murakami, J. Eur. Low Temperature Deposition of SnO2 Thin Films as Transparent Electrodes by Spray Pyrolysis of Tetra-n-butyltin(IV). J. Eur. Ceram. Soc., 21, pp.2099-2102.

14. T.W. Kim, D.U. Lee, D.C. Choo, J.H. Kim, H.J. Kim, J.H. Jeong, M. Jung, J.H. Bahang, H.L. Park, Y.S. Yoon, J.Y. Kim. Optical parameters in SnO2 nanocrystalline textured films grown on p-InSb (111) substrates. J. Phys. Chem. Solids 63, pp. 881-885 (2002).

15. F. Paraguay-Delgado, W. Antúnez-Flores, M. Miki-Yoshida, A. Aguilar-Elguezabal, P. Santiago, R. Diaz, J.A. Ascencio. Structural Analysis and growing mechanisms for long sno2 nanorods synthesized by spraypyrolysis. Nanotechnology, Vol. 16, 688 ,2005.

16. Raman Mishra P. K. Bajpai. Synthesis, Dielectric and Electrical Characterization of sno2nano-particle Prepared by Co-precipitation Method. Journal of International Academy of Physical Sciences Vol. 14 No.2, pp. 245-250, 2010.

17. Zhiwen Chen, J.K.L. Lai, C.H. Shek, and Haydn Chen. Synthesis and structural characterization of rutile sno2 nanocrystals. J. Mater. Res., Vol. 18, No. 6, Jun 2003.

18. M.M. Bagheri-Mohagheghia, N. Shahtahmasebia, M.R. Alinejada, A. Youssefic, M. Shokooh-Saremid. The effect of the post-annealing Temperature on the nano-structure and energy band gap of sno2 semiconducting oxide nano-particles synthesized by polymerizing–complexing sol–Gel method. Physica B, Vol. 403, pp. 2431–2437, 2008.

19. F. Du, Z. Guo, G. Li. Hydrothermal synthesis of sno2 hollow microspheres. Mater. Lett. Vol.59, pp. 2563,2005.

20. Y. Liu, E. Koep, M. Liu. A highly sensitive and fast-responding sno2 sensor fabricated by combustion chemical vapor deposition. Chem Mater, Vol. 17, pp. 3997, 2005.

21. M. Parthibavarman, V. Hariharan, C. Sekar. High-sensitivity humidity sensor based on SnO_2 nanoparticles synthesized by microwave irradiation method. Materials Science and Engineering C, Vol. 31, (2011), pp. 840-844, issue 5.

22. T. Krishnakumar, R. Jayaprakash, Nicola Pinna, V.N. Singh, B.R. Mehta, A.R. Phani. Microwave-assisted synthesis and characterization of flower shaped zinc oxide nanostructures. Materials Letters 63 (2), 242-245(2009).

23. Changesheng Liu, Yue Huang, Wei Shen, Jinghua Cui. Kinetics of Hydroxyapatite Precipitation at ph 10 to 11., Biomaterials, 22 (2001) 301-306. DOI: S0142-9612(00)00166-6

24. G.E. Patil, D.D. Kajale, P.T. Ahire, D.N. Chavan, N.K. Pawar, S.D. Shinde, V.B. Gaikwad, G.H. Jain: Synthesis, characterization and gas sensing Performance of sno2 thin films prepared by spray pyrolysis. Bull. Mater. Sci. 120, 1 (2011).

25. G.E. Patil, D.D. Kajale, V.B. Gaikwad, G.H. Jain. Nanocrystalline tin oxide thin Film as a low level H2S gas sensor. Int. J. Nanosci. 10, 1 (2011).